Optimal dynamics in a two-sector model with natural resources and foreign direct investments

Article *in* Applied Mathematics and Computation · October 2015

DOI: 10.1016/j.amc.2015.09.015

3 authors:

Angelo Antoci
Università degli Studi di Sassari
159 PUBLICATIONS **1,565** CITATIONS
SEE PROFILE

Paolo Russu
Università degli Studi di Sassari
76 PUBLICATIONS **624** CITATIONS
SEE PROFILE

Stefania Ragni
University of Ferrara
38 PUBLICATIONS **442** CITATIONS
SEE PROFILE

Optimal dynamics in a two-sector model with natural resources and foreign direct investments

Research · June 2015

CITATIONS
0

READS
46

3 authors:

Angelo Antoci
Università degli Studi di Sassari
139 PUBLICATIONS **1,253** CITATIONS
SEE PROFILE

Stefania Ragni
Università degli Studi di Sassari
35 PUBLICATIONS **341** CITATIONS
SEE PROFILE

Paolo Russu
Università degli Studi di Sassari
62 PUBLICATIONS **475** CITATIONS
SEE PROFILE

Optimal dynamics in a two-sector model with natural resources and foreign direct investments

Angelo Antoci[a], Stefania Ragni[a,*], Paolo Russu[a]

[a] *Department of Economics and Business*
University of Sassari Via Muroni 25, 07100 Sassari, Italy

Abstract

In this paper we analyze the optimal dynamics in an economy with three factors of production -labor, a renewable natural resource and physical capital- and two sectors -the "industrial sector" and the "local sector". External investors invest in the industrial sector as long as the return on the invested capital is higher than in the other economies. The activity of the industrial sector generates a negative impact on the environmental resource. In this context, we show that external investments may generate path-dependent economic dynamics. More specifically, three stationary states may coexist, two saddle points and a repellor. Furthermore, the time evolution of the stock of the environmental resource is monotonic; that is, a *U-shaped* path (i.e. the *environmental Kuznets curve*) cannot be observed along which the stock is initially decreasing and then becomes definitively increasing.

Keywords: foreign direct investment; two-sector economic growth model; environmental Kuznets curve; optimal management of environmental resources; optimal control problems.

1. Introduction

Industrialization processes and global integration of economies have increased the exposure of local rural communities to foreign direct investments. Unlike industrial activities, local production is usually very dependent on environmental dynamics. For local populations, natural systems represent means of subsistence or valuable economic services and assets. It has been estimated that in some large developing countries ecosystem services and other non-marketed goods account for a part of the source of livelihood of rural and forest-dwelling poor households wich is between the 47 percent and the 89 percent on the whole. In these frameworks, local activities are exposed to multiple sources of pollution produced by the external investors. The unsustainable management of natural resources in local activities can trigger a vicious circle of poverty and environmental degradation. Indeed, the struggles of local communities against external agents, which threaten the environment, increase all over the world; that fact suggests that this interaction may not be insignificant. Many grassroots protests are against environmental degradation caused by extractive, fishery and agriculture activities of large firms. Case studies of struggles by poor communities, to gain control over the natural resources and to deal with injustice and environmental degradation created by the big companies, have been documented for instance in [1] and [2]. Since the late Eighties, the impact on poverty and deforestation produced by the expansion of large mechanized agriculture, livestock and timber activities has been analyzed in [3], [4] and, more recently, in [5]. In other cases, local communities are negatively affected by processes of industrialization and urbanization. China provides some of the most symbolic examples of rural communities harmed by

*Corresponding author: Dipartimento di Scienze Economiche e Aziendali, Università di Sassari, Via Muroni 25, 07100 Sassari Italy Tel.+39 079 213016 - Fax +39 079 203002

Email addresses: angelo.antoci@virgilio.it (Angelo Antoci), sragni@uniss.it (Stefania Ragni), russu@uniss.it (Paolo Russu)

the arrival of new manufacturing firms. Heavy damages to agriculture and fishery sectors caused by Chinese industrialization have been documented, among the others, by [6], [7] and [8]. Other examples are provided by textile activities in India. As shown by [9] for Tamil Nadu, the promotion of investments in this sector is accompanied by a devastating industrial pollution which is causing an increasing loss of water and agriculture productivity and a reduction in the cultivable area. One of the possible mechanisms according to which the industrialization processes may negatively affect local communities has been highlighted by some recent theoretical works focused on the undesirable effects of the industrialization processes (see, e.g., [10], [11], [12], [13]). According to this literature, the environmental degradation -caused by the industrial production- may be an engine of welfare-reducing economic growth. The vicious mechanism can be summarized as follows: 1) the industrial activities cause environmental degradation and a consequent reduction in labor productivity in natural resource-dependent sectors (agriculture, tourism and so on); 2) the reduction in labor productivity in these sectors incentives individuals to work in the industrial sector as waged workers; this causes a reduction in equilibrium wages in the industrial sector and a consequent expansion of the industrial activity; 3) the increase in industrial production causes further environmental degradation which, in turn, gives rise to a further expansion of the industrial sector and so on.

As a difference with the above cited theoretical literature, our paper focuses on the positive effects that the external capital inflows may produce, even though these flows encourage the expansion of an industrial sector which generates a negative impact on environmental resources. We develop a dynamic model describing the links between local communities and external investments, including the negative environmental impact and the job effect of external capital inflows. In our model, the effect of poverty-reduction of external capital flows operates through the labor market by creating new labor opportunities in the industrial sector. Our work is complementary to that of [13], where external investment inflows may generate a self-enforcing growth process related to an increase in local agents' poverty. Indeed, we analyze an economy with the same features; however, as a difference with respect to the analysis developed in [13], we assume that individuals' labor allocation choices are determined by a benevolent social planner who has the objective of maximizing individuals' welfare. In this context, we aim at pointing out those conditions which allow the external investments to generate an increase in welfare. More specifically, we show how the optimal labor allocation choices are related to the pollution rate of the industrial sector and to the carrying capacity of the environmental resources. Even though we consider a very simple framework, the dynamics generated by our model may exhibit multiplicity of saddle point stable stationary states. This implies that the expansion of the industrial sector, which in our model is strictly related to the labor allocation choices of the local community, may be a path-dependent process.

The article is organized as follows. Section 2 presents the model; sections 3 and 4 investigate the basic properties of dynamics that emerge from the model; section 5 deals with the numerical methods used to approximate solutions and section 6 provides the results of some numerical tests; section 7 concludes.

2. The model setup

We study the dynamics of an economy where the production activities depend on three factors of production: labor, a renewable natural resource and physical capital. In this economy there are two sectors, the "industrial sector" and the "local sector", and economic agents belong to two different communities, the "External Investors" (I-agents) and the "Local Agents" (L-agents). We assume that I-agents invest in the industrial sector and do not face credit constraints; that is, they invest in this economy as long as the return on the produced capital is higher than the ones in the other economies. The I-agents also hire the labor force provided by the L-agents. In this respect, the L-agents use their own working capacity partly working as employees for the I-agents and partly in the local sector, where they directly exploit the natural resource. In order to fix our ideas, the local sector can be considered as the farming one, even though it may include fishery, forestry or also tourism. On the other hand, the industrial sector includes all the activities which are intensive in physical capital and generate a negative impact on the environmental resource.

This is a stylized scenario, but it can represent the main differences among the sets of options that local populations and external investors can use to generate their income flows and to protect themselves from environmental degradation. The use of intensive labor techniques, employment of family labor and constraints in access to credit markets are often crucial features for the production activities of local communities. For instance, [14] summarizes a review of empirical literature about the relationship between poverty and natural resource in developing countries by observing that the rural poor are almost "assetless". They depend "critically on the use of common-property and open access resources for their income", they rely on small plots of lands and on selling their labor which is their only other asset. As in [15], we model these settings by excluding that the local agents can accumulate physical capital and by assuming that they can rely on two productive inputs, namely their labor and natural capital.

By contrast, external investors usually manage intensive capital activities based on the employment of wage labor and their companies or firms are able to gain access to capital markets. In addition, their production is characterized by a high degree of mobility; indeed, it relies on wage labor, which is also available in other economies, and on physical capital, that can be employed elsewhere. Moreover the external investors can defend themselves against a reduction in capital returns in the local economy by moving their capital towards other economies.

Both populations of economic agents are represented by a continuum of identical individuals and the size of each community is equal to 1. In this respect, we may deal with a "representative" L-agent and a "representative" I-agent. We assume that the production functions of the two sectors are concave, increasing and homogenous of degree 1 with respect to their inputs. In particular, the production function of the representative L-agent is given by

$$Y_L = E^{\alpha} L^{1-\alpha},$$

where E is the stock of the free access environmental resource, L represents the amount of time the representative L-agent spends on local sector production and the parameter α satisfies the condition $0 < \alpha < 1$.
The production function of the representative I-agent depends on the investment in physical capital K_I and is defined by the following

$$Y_I = \delta K_I^{\gamma} (1 - L)^{1-\gamma}, \tag{1}$$

where the term $1 - L$ represents the L-agent's labor employed by the representative I-agent as wage work, $\delta > 0$ is a productivity parameter and $1 > \gamma > 0$.
The time evolution of the stock E is described by

$$\dot{E} = E(\overline{E} - E) - \eta Y_I, \tag{2}$$

where η is a positive parameter which measures the environmental impact caused by the industrial output Y_I. The positive parameter $\overline{E}$ represents the carrying capacity of the environmental resource, that is the value that E would approach in absence of the negative effect generated by the industrial sector. We do not account for the environmental impact of the local sector, since we focus on those scenarios where the environmental damage of the local agent production is negligible compared to that of the industrial sector.

In this framework, the representative I-agent chooses her labor demand $1-L$ and the investment in physical capital K_I in order to maximize the profit function

$$\Pi_I = \delta K_I^{\gamma} (1 - L)^{1-\gamma} - w(1 - L) - rK_I,$$

where r and w represent the rental rate of K_I (which can be also interpreted as an opportunity cost) and the wage rate, respectively. Both w and r are considered as exogenously determined by the representative I-agent. By the way, the wage w is endogenously set in the economy under the assumption that the labor market is always in equilibrium, while $r > 0$ is considered an exogenous parameter whose value is determined in the international markets. We assume that the inflow of K_I is potentially unlimited and, as a consequence, the dynamics of K_I is not linked to the I-agents' savings but only to the productivity of K_I (which, in turn, depends on L and K_I). More

specifically, the representative I-agent chooses L and K_I in order to maximize, in each instant of time, her revenues Π_I; this gives rise to the following first order conditions

$$\frac{\partial \Pi_I}{\partial (1-L)} = \delta(1-\gamma) K_I^{\gamma} (1-L)^{-\gamma} - w = 0, \tag{3}$$

$$\frac{\partial \Pi_I}{\partial K_I} = \delta \gamma K_I^{\gamma-1} (1-L)^{1-\gamma} - r = 0. \tag{4}$$

Notice that, according to equation (4), the following relationship holds

$$K_I = \left(\frac{\gamma\delta}{r}\right)^{\frac{1}{1-\gamma}} (1-L). \tag{5}$$

This means that the investment K_I of the I-agent in the industrial sector is proportional to the labor input $1-L$.

The revenues of the representative L-agent are given by

$$\Pi_L = E^{\alpha} L^{1-\alpha} + w(1-L).$$

It is not so difficult to prove that the term w can be obtained by means of the other parameters δ, γ and r, thus the revenues Π_L depends only on terms E and L. Indeed, we notice that the representative I-agent chooses $1-L$ and K_I which satisfy the first order conditions (3) and (4); therefore, we replace (5) into (3) and obtain the value of the equilibrium wage rate w given by

$$w = \delta(1-\gamma) \left(\frac{\delta\gamma}{r}\right)^{\frac{\gamma}{1-\gamma}}.$$

This relationship can be exploited in Π_L in order to have

$$\Pi_L(E(t), L(t)) = E(t)^{\alpha} L(t)^{1-\alpha} + a(1-\gamma)(1-L(t)), \tag{6}$$

where we set $a = \delta \left(\frac{\delta\gamma}{r}\right)^{\frac{\gamma}{1-\gamma}}$. In addition, we employ (5) in (2) and obtain

$$\dot{E}(t) = f(L(t), E(t)),$$

with $f(L,E) := E(\overline{E} - E) - \eta a(1-L)$. In this framework, the social planner has to choose the function $L(t)$, $t \in [0, +\infty)$, that maximizes the revenues $\Pi := \Pi_L$ defined in (6) and solves the following optimal control problem:

$$\max_{L} \int_0^{+\infty} e^{-\sigma t} \Pi(L(t), E(t))\, dt, \tag{7}$$

subject to

$$\begin{aligned} &\dot{E}(t) = f(L(t), E(t)), \qquad t \geq 0, \\ &0 \leq L(t) \leq 1, \qquad t \geq 0, \\ &E(t) \geq 0, \qquad t \geq 0, \qquad E(0) = E_0 \geq 0, \end{aligned}$$

where the parameter $\sigma > 0$ represents the discount rate.

3. Optimal economic dynamics

We consider the interval $U = [0,1]$, which represents the admissible set for the control variable. According to the sign of function $f(L,E)$ which defines the dynamics for $E(t)$ in correspondence with each $L \in U$, it is not so difficult to verify that the state variable is bounded from above by

the constant value $C_0 = \max\{\overline{E}, E_0\}$, i.e.

$$0 \leq E(t) \leq C_0, \tag{8}$$

for each $t \geq 0$. We set $X = [0, C_0]$. Moreover, in Appendix A.1 we prove that the following properties hold:

(P1) For arbitrary $T > 0$ there is the closed set X such that for any admissible trajectory $E(\cdot)$ of problem

$$\dot{E} = f(L, E), \qquad L \in U,$$

its values $E(t)$ belong to X for all $t \in [0, T]$.

(P2) There exists the constant value $\overline{E} \geq 0$ such that the product $E \cdot f(L, E)$ satisfies the relationship

$$E \cdot f(L, E) \leq \overline{E}(1 + E^2), \qquad \text{for any} \quad L \in U, \quad E \in X.$$

(P3) For each $E \in X$, the function $L \to f(L, E)$ is affine in control variable L, indeed it has the form

$$f(L, E) = f_0(E) + f_1(E)L, \qquad \text{for all} \quad L \in U, \quad E \in X,$$

where $f_0 : X \longrightarrow \mathbb{R}$ and $f_1 : X \longrightarrow \mathbb{R}$ are constinuously differentiable.

(P4) The set U is a convex compactum in $\mathbb{R}$.

(P5) For any fixed $E \in X$, the function $L \to \Pi(L, E)$ is concave in variable L.

(P6) There exist positive functions ν and ω on $[0, +\infty)$ such that $\nu(t) \to 0$ and $\omega(t) \to 0$ as $t \to +\infty$ and, for every admissible pair $(L(\cdot), E(\cdot)) \in U \times X$, the following inequalities hold

$$e^{-\sigma t} \max_{L \in U} |\Pi(L, E(t))| \leq \nu(t), \qquad \text{for any} \quad t \geq 0,$$

$$\int_T^{+\infty} e^{-\sigma t} |\Pi(L(t), E(t))| \, dt \leq \omega(T), \qquad \text{for any} \quad T \geq 0.$$

The previous conditions (P1)-(P6) assure the existence of an optimal admissible control L in problem (7) (see Theorem 15 in [16] as properties (P1)-(P6) are equivalent to assumptions (A1), (A2), (A5) and (A6) in that paper). Moreover, under the same conditions, the "core" of the maximum principle can be applied in order to provide the necessary optimality conditions (see Theorem 17 in [16]). More precisely, we define the current value Hamiltonian

$$\mathcal{H}(L, E, \lambda) = \Pi(L, E) + \lambda f(L, E),$$

where λ represents the current value of costate variable. Then, we state necessary conditions for the optimal trajectories $L(t)$, $E(t)$:

$$\dot{E}(t) = \frac{\partial \mathcal{H}}{\partial \lambda}(L(t), E(t), \lambda(t)), \tag{9}$$

$$\dot{\lambda}(t) = \sigma\lambda(t) - \frac{\partial \mathcal{H}}{\partial E}(L(t), E(t), \lambda(t)), \tag{10}$$

where control variable $L(t) \in U$, at each time t, is obtained as the solution of the optimization problem

$$\mathcal{H}(L(t), E(t), \lambda(t)) = \max_{L \in U} \mathcal{H}(L, E(t), \lambda(t)). \tag{11}$$

For the sake of completeness, we also point out that the so-called normal-form stationarity condition holds

$$\max_{L \in U} \mathcal{H}(L, E(t), \lambda(t)) = \sigma \int_t^{+\infty} e^{-\sigma s} \Pi(L(s), E(s)) \, ds,$$

for any $t \geq 0$. Assuming problem (11) has got an interior admissible solution (i.e. $0 < L(t) < 1$ at each t), then the first order optimality condition

$$\frac{\partial \mathcal{H}}{\partial L}(L(t), E(t), \lambda(t)) = 0,$$

has to be satisfied; thus we have

$$(1-\alpha)\left(\frac{E(t)}{L(t)}\right)^{\alpha} - a(1-\gamma) + \eta a \lambda(t) = 0.$$

In this respect, the control variable can be obtained as a function of the remaining variables according to

$$L(t) = \left(\frac{1-\alpha}{a(1-\gamma) - \eta a \lambda(t)}\right)^{\frac{1}{\alpha}} E(t). \tag{12}$$

The evolution dynamics for the state and the costate variables can be explicitly written as

$$\begin{aligned} \dot{E}(t) &= E(t)(\overline{E} - E(t)) - \eta a (1 - L(t)), \\ \dot{\lambda}(t) &= (\sigma - \overline{E} + 2E(t))\lambda(t) - \alpha \left(\frac{L(t)}{E(t)}\right)^{1-\alpha}, \end{aligned}$$

where the initial condition $E(0) = E_0$ is known for the state $E(t) \geq 0$.

Remark 1. *As an alternative, in the case when problem (11) is solved by $L(t) = 1$ for t in a suitable time interval, then the optimality condition yields*

$$(1-\alpha)E(t)^{\alpha} - a(1-\gamma) + \eta a \lambda(t) \geq 0,$$

and system (9)-(10) is given by

$$\begin{aligned} \dot{E}(t) &= E(t)(\overline{E} - E(t)), \\ \dot{\lambda}(t) &= (\sigma - \overline{E} + 2E(t))\lambda(t) - \alpha E(t)^{\alpha - 1}. \end{aligned}$$

Moreover, in the remaining possible case, if $L(t) = 0$ represents a solution to problem (11) in a suitable time interval, then it is possible to state the existence of a neighborhood $(0, \varepsilon)$ of the origin where

$$(1-\alpha)\left(\frac{E(t)}{l}\right)^{\alpha} - a(1-\gamma) + \eta a \lambda(t) \leq 0, \qquad \text{for all } l \in (0, \varepsilon).$$

In that case, the dynamic system for the state and costate variables can be written as

$$\begin{aligned} \dot{E}(t) &= E(t)(\overline{E} - E(t)) - \eta a, \\ \dot{\lambda}(t) &= (\sigma - \overline{E} + 2E(t))\lambda(t). \end{aligned}$$

We would point out that the model we are dealing with is non-concave. It is evident that it cannot be solved in closed form. In this respect, as a first step, a qualitative analysis of the solution may be performed; indeed it is possible and convenient investigating the existence and the features of possible stationary equilibria for the dynamical system which describes the first order optimality conditions related to the problem. As a second step, the numerical approach represents the only means to confirm the qualitative results and to develop a quantitative analysis of the model.

4. Qualitative analysis of the stationary states

The long-run behavior of the solution may be analyzed by studying the existence and the nature of stationary states for the dynamical system (9)-(10), which is related to the necessary optimality conditions. We focus on the stationary state analysis for inner values of the control variable (i.e.

$0 < L(t) < 1$). For the sake of simplicity, we perform a change of variable and set

$$z(t) = \left(\frac{1-\alpha}{a(1-\gamma-\lambda(t)\eta)} \right)^{\frac{1}{\alpha}};$$

therefore, we have $L(t) = z(t)E(t)$ in (12). It is not so difficult to verify that the dynamics for $E(t)$ and $z(t)$ are described by equations

$$\dot{E}(t) = F(z(t), E(t)), \tag{13}$$
$$\dot{z}(t) = G(z(t), E(t)), \tag{14}$$

where

$$\begin{aligned} F(z,E) &= E(\overline{E} - E) - \eta a\,(1 - zE)\,, \\ G(z,E) &= \frac{z}{\alpha(1-\alpha)} \left((\sigma - \overline{E} + 2E)((1-\gamma)az^{\alpha} - (1-\alpha)) - \alpha\eta az \right). \end{aligned}$$

Our interest is focused on the existence of equilibrium points of the previous differential problem; then, we search for the solutions z^*, E^* of the nonlinear system

$$\begin{aligned} F(z^*, E^*) &= 0, \\ G(z^*, E^*) &= 0, \end{aligned}$$

in the admissible region in $\mathbb{R}^2$ where $0 < L(t) < 1$ and $E(t) > 0$. From this requirement, we obtain $z^* > 0$, $E^* > 0$, $1 - z^*E^* > 0$ and $E^*(\overline{E} - E^*) > 0$ (arising from $\dot{E}(t) = 0$)). These relationships yield the following result.

Proposition 1. *Any inner admissible equilibrium point (z^*, E^*) for system (13)-(14) lies in the region of the (z, E)-plane defined by*

$$\Omega = \{(z, E) \in \mathbb{R}^2 \mid z > 0,\ 0 < E < \overline{E},\ 1 - zE > 0\}.$$

In this framework, we define $\mathcal{C}_F$ and $\mathcal{C}_G$ as the curves in the phase plane (z, E) where $F(z, E) = 0$ and $G(z, E) = 0$, respectively. Their crossing points in Ω represent the equilibria of interest. Therefore, we are going to analyze the shapes for the branches of both $\mathcal{C}_F$ and $\mathcal{C}_G$ which lie in the admissible region Ω. In the sequel, we set

$$\bar{z} = \left(\frac{1-\alpha}{a(1-\gamma)} \right)^{\frac{1}{\alpha}}, \quad \widehat{z} = \frac{2\sqrt{a\eta} - \overline{E}}{a\eta}, \quad \widetilde{z} = \frac{\bar{z}}{1-\alpha} = \left(\frac{1}{a(1-\gamma)} \right)^{\frac{1}{\alpha}},$$

and we denote by $\mathcal{C}$ the curve where $1 - zE = 0$, which defines Ω.

Furthermore, we recall the economic interpretation of the costate variable $\lambda(t)$ as the "shadow price" of the environmental resource stock $E(t)$ at each time t (see, for instance, [16]). For that reason, we only focus on the non-negative values for λ on the long-run; a negative value of λ would imply that an increase in the initial stock $E(0) = E_0$ generates a reduction in the maximized value of the objective function in (7). It follows that, under conditions $z^* > 0$, $\lambda(t) > 0$ and $\dot{\lambda}(t) = 0$ at the equilibrium, then $\sigma - \overline{E} + 2E^* > 0$. Therefore, the relationship $\dot{z}(t) = 0$ is exploited and the admissible region for the stationary states reduces to the following set

$$\overline{\Omega} = \{(z, E) \in \mathbb{R}^2 \mid z > \bar{z},\ 0 < E < \overline{E},\ 1 - zE > 0\},$$

in the phase plane (z, E). In this respect, we focus on the possible crossing points between $\mathcal{C}_F$ and $\mathcal{C}_G$ in the reduced admissible region $\overline{\Omega}$. Thus, we are going to discuss some features of both curves:

- As a first step, we notice that $\mathcal{C}_F$ represents an hyperbola whose asymptotes are featured by equations $E = 0$ and $E = a\eta z + \overline{E}$. The branch in $\overline{\Omega}$ has got vertex V with coordinates $z = \widehat{z}$ and $E = \sqrt{a\eta}$; moreover, the point with $z = 1/\overline{E}$ and $E = \overline{E}$ belongs to both $\mathcal{C}_F$ and $\mathcal{C}$. In addition, $\mathcal{C}_F$ lies always under $\mathcal{C}$ in the region $\overline{\Omega}$, as it is shown in Figure 1, where

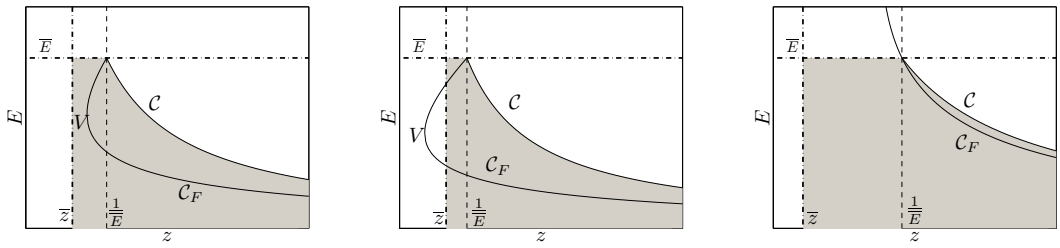

Figure 1: The path of the curve $\mathcal{C}_F$ in the reduced admissible region for the stationary states, which is represented by the grey area. On the left-hand side we show the case when the vertex V lies in $\overline{\Omega}$. In the middle and on the right side we have other cases when V is outside.

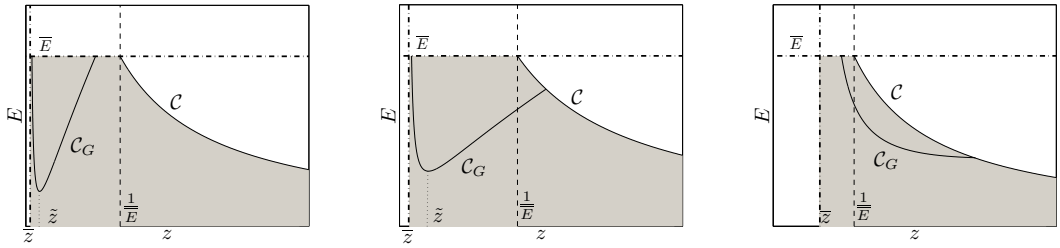

Figure 2: Possible paths of the curve $\mathcal{C}_G$ in the reduced region $\overline{\Omega}$, which is represented by the grey area. On the left-hand side and in the middle we show the case when the local minimum point $(\widetilde{z}, \varphi(\widetilde{z}))$ lies in $\overline{\Omega}$ (i.e. $\widetilde{z} < 1/\overline{E}$ and $\varphi(\widetilde{z}) < \overline{E}$); on the right side we have the case when the same minimum is outside (i.e. $1/\overline{E} < \widetilde{z}$ and $1/\widetilde{z} < \varphi(\widetilde{z}) < \overline{E}$).

three different cases are considered. On the left-hand side of the figure the vertex V is in the admissible region, that happens when $\bar{z} < \widehat{z}$ and $\sqrt{a\eta} < \overline{E}$; the middle part and the right-hand side of the figure concern other cases when V is outside. Precisely, in the middle of the figure, we assume that $\widehat{z} < \bar{z}$ and $\sqrt{a\eta} < \overline{E}$; on the right-hand side we suppose that $\widehat{z} < 1/\overline{E}$ and $\overline{E} < \sqrt{a\eta}$.

- As a second step, we account for the path of the curve $\mathcal{C}_G$: we write the variable E as a function of z and set $E = \varphi(z)$ with

$$\varphi(z) = \frac{\overline{E} - \sigma}{2} + \frac{1}{2}\frac{\alpha\eta a z}{(1-\gamma)az^{\alpha} - (1-\alpha)}.$$

It is evident that $\varphi(z)$ is defined for $z \geq 0$ and it has got a vertical asymptote in the line $z = \bar{z}$. In addition, the function $\varphi(z)$ is featured by a local minimum value, which is reached for $z = \widetilde{z}$ (remark that $\bar{z} < \widetilde{z}$ and $\varphi(\widetilde{z}) = (\overline{E} - \sigma + \eta a\widetilde{z})/2$). Then, it is easy to verify that $\varphi(z)$ is convex and diverges at $z \to +\infty$.
In Figure 2 we show how some possible path of $\mathcal{C}_G$ may be in the reduced admissible region for the stationary states. On the left-hand side and in the middle of the figure, we have the local minimum point that lies in $\overline{\Omega}$. As an alternative, on the right side we assume that $1/\widetilde{z} < \varphi(\widetilde{z}) < \overline{E}$ (that also yields $1/\overline{E} < \widetilde{z}$), then the same minimum point is outside and the path for $\mathcal{C}_G$ always decreases.

Under the previous reasoning, we argue it may happen that the curves $\mathcal{C}_F$ and $\mathcal{C}_G$ have no points in common in the region of interest. As the alternative case, assuming that $\mathcal{C}_F$ crosses $\mathcal{C}_G$ in $\overline{\Omega}$, then we may have up to four crossing points; really, in the next proposition we prove that the maximum number of stationary states is allowed to be three.

Proposition 2. *The optimal control model may have no more than three inner stationary states.*

Proof. It is evident that the curve $\mathcal{C}_F$ can be splitted into two different branches, which are described by the equations

$$E = \varphi_{up}(z), \qquad E = \varphi_{dw}(z), \qquad \text{for } z \geq \widehat{z},$$

where

$$\varphi_{up}(z) = \frac{\overline{E} + a\eta z + \sqrt{(\overline{E} + a\eta z)^2 - 4a\eta}}{2}, \quad \varphi_{dw}(z) = \frac{\overline{E} + a\eta z - \sqrt{(\overline{E} + a\eta z)^2 - 4a\eta}}{2}.$$

We notice that the first branch represents the part of the curve which is over the line $E = \sqrt{a\eta}$; thus, the second one is the part of $\mathcal{C}_F$ under the same line. The curve $\mathcal{C}_G$ may cross both the upper and the lower branches of $\mathcal{C}_F$ for z in $[\overline{z}, \widetilde{z}]$. It follows that, the number of possible stationary states (z^*, E^*) with $\overline{z} < z^* < \widetilde{z}$ may be not greater than two. It is evident that a necessary condition for the existence of any stationary state in the strip defined by $[\overline{z}, \widetilde{z}]$ (i.e. $\overline{z} < z^* < \widetilde{z}$) is

$$\widehat{z} < \widetilde{z} < \frac{1}{\overline{\overline{E}}}, \quad \text{and} \quad \sqrt{a\eta} < \overline{E}. \tag{15}$$

On the other hand, we are going to prove that the curve $\mathcal{C}_G$ cannot cross the upper branch of $\mathcal{C}_F$ through any point (z, E) with $z > \widetilde{z}$, in the case when (15) holds. Indeed, assuming that a crossing point appears, then it would be unique and the function $d(z) = \varphi_{up}(z) - \varphi(z)$ should perform only one change in its sign for $z \in [\widetilde{z}, 1/\overline{E}]$. Notice that $d(z)$ has the same sign of

$$D(z) = (1-\gamma)(z^\alpha - \overline{z}^\alpha)\left(\sigma + a\eta z + \sqrt{(\overline{E} + a\eta z)^2 - 4a\eta}\right) - \alpha\eta z, \qquad \widetilde{z} < z < \frac{1}{\overline{\overline{E}}}.$$

In this respect, since $\widetilde{z}^\alpha - \overline{z}^\alpha = \alpha/(a(1-\gamma))$, we have

$$D(\widetilde{z}) = \frac{\alpha}{a}\left(\sigma + \sqrt{(\overline{E} + a\eta\widetilde{z})^2 - 4a\eta}\right) > 0.$$

Moreover, relationship $\overline{z}^\alpha = (1-\alpha)/(a(1-\gamma))$ may be exploited in order to obtain

$$D\left(\frac{1}{\overline{\overline{E}}}\right) = (1-\gamma)\left(\left(\frac{1}{\overline{\overline{E}}}\right)^\alpha - \overline{z}^\alpha\right)T(\overline{E}) + (1-\gamma)\left(\left(\frac{1}{\overline{\overline{E}}}\right)^\alpha - \frac{1-\alpha}{a(1-\gamma)}\right)a\eta\frac{1}{\overline{\overline{E}}} - \alpha\eta\frac{1}{\overline{\overline{E}}},$$

where we set $T(\overline{E}) = \sigma + \sqrt{(\overline{E} + a\eta\overline{E})^2 - 4a\eta} > 0$. Therefore, the following relationship holds

$$D\left(\frac{1}{\overline{\overline{E}}}\right) = (1-\gamma)\left(\left(\frac{1}{\overline{\overline{E}}}\right)^\alpha - \overline{z}^\alpha\right)T(\overline{E}) + \frac{\eta a(1-\gamma)}{\overline{E}}\left(\left(\frac{1}{\overline{\overline{E}}}\right)^\alpha - \widetilde{z}^\alpha\right) > 0.$$

It follows that the sign of function $d(z)$ does not change for $z \in [\widetilde{z}, 1/\overline{E}]$; as a consequence, no crossing point may exist between $\mathcal{C}_G$ and the upper branch of $\mathcal{C}_F$ in the region of $\overline{\Omega}$ where $z > \widetilde{z}$. Anyway the curve $\mathcal{C}_G$ may cross the lower branch of $\mathcal{C}_F$ once in the same region of $\overline{\Omega}$. Thus, the result is completely proved. ■

For the sake of completeness we would remark that, when three equilibria arise, they lie in the admissible region as it is shown in the plots of Figure 3 and correspond to the points marked as A, B and C. Two different locations are possible: they are shown in Figures 3(a) and 3(b). In addition, Figure 3(c) represents the zoom of the red square in Figure 3(b). As it is explained in the previous proof, it is evident that two points, B and C, are located on the lower branch of $\mathcal{C}_F$; on the contrary, the first point A may lie either on the upper branch or on the lower part of the same curve.

In that framework, we provide some sufficient conditions for the existence of stationary states in the following proposition.

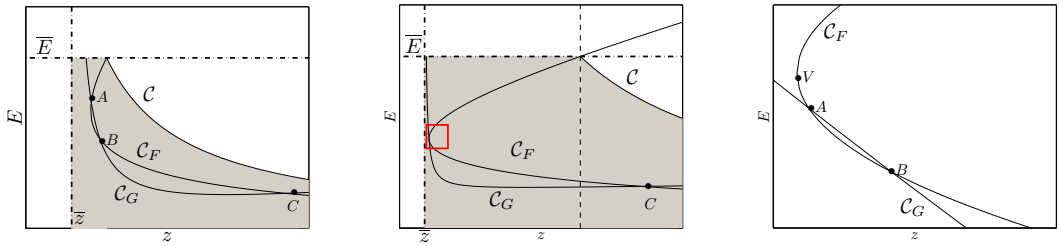

(a) (b) (c)

Figure 3: Possible locations of three equilibria in the admissible region $\overline{\Omega}$ in plots 3(a) and 3(b). Picture 3(c) represents the zoom of the red square in plot 3(b).

Proposition 3. *We assume that*

$$\widetilde{z}\overline{E} = 1, \tag{16}$$

$$\sigma = \overline{E} + \eta a \widetilde{z}, \tag{17}$$

$$\eta < \left(\frac{1 - \sqrt{1 - (1-\alpha)^{\frac{1}{\alpha}}}}{\widetilde{z}\sqrt{a}(1-\alpha)^{\frac{1}{\alpha}}} \right)^2. \tag{18}$$

Then three inner stationary states exist in the admissible region $\overline{\Omega}$.

The proof is developed in Appendix A.2.

4.1. Stability analysis

Concerning the analysis and stability of the stationary points, we consider the Jacobian matrix of system (13)-(14). Precisely, it is evaluated at any stationary state (z^*, E^*) as

$$\mathcal{J}^* = \begin{pmatrix} F_E(z^*, E^*) & F_z(z^*, E^*) \\ G_E(z^*, E^*) & G_z(z^*, E^*) \end{pmatrix} \tag{19}$$

where

$$F_E(z^*, E^*) = \overline{E} - 2E^* + \eta a z^*, \qquad F_z(z^*, E^*) = \eta a \overline{E},$$

$$G_E(z^*, E^*) = \frac{2az^*(1-\gamma)((z^*)^\alpha - \overline{z}^\alpha)}{\alpha(1-\alpha)},$$

$$G_z(z^*, E^*) = \frac{(\sigma - \overline{E} + 2E^*)(1-\gamma)a((\alpha+1)(z^*)^\alpha - \overline{z}^\alpha) - 2\alpha\eta a z^*}{\alpha(1-\alpha)}.$$

It is well-known that the study of the eigenvalues of $\mathcal{J}^*$ is crucial in order to understand the nature of the stationary state we are accounting for. In this respect, the characteristic polynomial of the Jacobian matrix is

$$\mathcal{P}(\lambda) = \lambda^2 - \mathcal{T}\lambda + \mathcal{D},$$

where $\mathcal{T} = F_E(z^*, E^*) + G_z(z^*, E^*)$ and $\mathcal{D} = F_E(z^*, E^*)G_z(z^*, E^*) - F_z(z^*, E^*)G_E(z^*, E^*)$ represent the trace and the determinant of $\mathcal{J}^*$, respectively.
It is evident that both roots of $\mathcal{P}(\lambda)$ are real[1] and their signs depend on the coefficients $\mathcal{T}$ and $\mathcal{D}$. For instance, under the assumption that $\mathcal{T} > 0$ and $\mathcal{D} > 0$, both roots are negative and the stationary state (z^*, E^*) represents a repellor; whereas, when $\mathcal{D} < 0$, then the roots have opposite sign and the stationary state is a saddle point.
That kind of analysis can be carried out by investigating the slope of both curves $\mathcal{C}_F$ and $\mathcal{C}_G$ at

[1]It is not so difficult to verify that the discriminant for $\mathcal{P}(\lambda) = 0$ is $d = (F_E(z^*, E^*) - G_z(z^*, E^*))^2 + 4F_z(z^*, E^*)G_E(z^*, E^*) > 0$, since $F_z(z^*, E^*) > 0$ and $G_E(z^*, E^*) > 0$.

their crossing points in order to evaluate the signs of $\mathcal{T}$ and $\mathcal{D}$. The corresponding results are provided in the following proposition.

Proposition 4. *Suppose that three stationary states $A(z_A^*, E_A^*)$, $B(z_B^*, E_B^*)$, $C(z_C^*, E_C^*)$ exist, with $z_A^* < z_B^* < z_C^*$. Then A and C are saddle points while B is a repellor.*

The proof is given in Appendix A.3. We would like to remark that the same argument, which is developed to prove the previous result, may be employed in order to investigate the stability when there exist less than three stationary states.

5. Approximation of the solution

Our aim consists of discretizing the continuous model by means of different numerical schemes in order to approximate the solution and provide some numerical results which may validate the theoretical analysis we have carried out so far. In addition, the numerical tool represents a means for analyzing some economical features of the solution, as it will be shown in the next Section 6.

In this respect, we adopt different numerical procedures to solve the problem. Actually, the first approach consists of finding a solution that satisfies optimality necessary conditions in a classical way; in that sense, it represents a so-called "indirect method". It searches for the stable paths of the stationary states by means of the so-called backward integration. As an alternative, another numerical approach is also exploited; it is a "direct method" which achieves the solution through the direct optimization of the objective function. Indeed, the optimal control model is converted by suitable discretization into a nonlinear programming problem, where the nodal values for the control parameters represent the optimization variables and the state is recursively approximated by specific Runge-Kutta methods. In this way, it provides the time evolution of the involved variables in a direct way. In the sequel, we describe these numerical schemes.

We notice that the methods have different features. For instance, the first one is less expensive since it requires the numerical integration of a differential system; by contrast, the direct procedure has a heavier computational cost as it involves the solution of a discrete optimization problem. Anyway, the indirect approach exploits the necessary optimality conditions which are satisfied by maximizers and minimizers, as well as points that are not optimizers, then there is no reason, in general, to expect a solution to be the required optimum. On the other hand, the second method overcomes this drawback and approximates the time evolution of the involved variables in a direct way.

We would remark that, concerning the numerical simulations we provide in Section 6, the results in the (z, E) phase-plane obtained by means of both approaches are in agreement. In that sense, the use of different procedures which provide the same discrete approximations confirms and validates our results.

5.1. The "indirect method" description

The main idea of the method would be the numerical integration of system (13)-(14) fulfilled by initial conditions

$$E(0) = E_0, \qquad z(0) = z_0.$$

The aim consists of finding the equilibria of the given system and evaluating their stable paths. In this respect, it is evident that the value E_0 is given in the model, but the other value z_0 is not a-priori known. The problem may be solved by means of the method which we are going to describe and deals with the so-called backward integration (see [17]).

More precisely, we consider a given admissible stationary state (z^*, E^*) and recall that the evolution dynamics is well approximated by the linearized system

$$\begin{pmatrix} \dot{E}(t) \\ \dot{z}(t) \end{pmatrix} = \mathcal{J}^* \begin{pmatrix} E(t) \\ z(t) \end{pmatrix},$$

in a suitable neighborhood of the point itself. We assume that the equilibrium (z^*, E^*) represents a saddle point (Proposition 4 provides the sufficient conditions for the existence of two saddle points). Then, it is well-known that the invariant sets for the linear system are the eigenspaces of the Jacobian matrix $\mathcal{J}^*$. In particular, the stable set is given by the eigenspace $\mathcal{S}^s$ of the

negative eigenvalue and the unstable set is represented by the eigenspace $\mathcal{S}^u$ related to the positive eigenvalue of $\mathcal{J}^*$. It is evident that both spaces are one-dimensional and linear.

As what concerns the more general analysis of the nonlinear system, we denote by

$$\phi^t(\breve{z}, \breve{E}) = (z(t), E(t)),$$

the flow that transforms the initial state $(\breve{z}, \breve{E})$ into the solution $(z(t), E(t))$ of (13)-(14) at time t. The Manifold Theorem (see, among the others, [18], [19], [20]) assures that there exist local stable and unstable manifolds $\mathcal{W}^s_{loc}$ and $\mathcal{W}^u_{loc}$, which have the same dimension of $\mathcal{S}^s$ and $\mathcal{S}^u$ and are tangent to them at (z^*, E^*), such that

$$\mathcal{W}^s_{loc} = \left\{ (\breve{z}, \breve{E}) \in U^* \ : \ \lim_{t\to\infty} \phi^t(\breve{z}, \breve{E}) = (z^*, E^*), \text{ and } \phi^t(\breve{z}, \breve{E}) \in U^*, \ t \geq 0 \right\},$$

and

$$\mathcal{W}^u_{loc} = \left\{ (\breve{z}, \breve{E}) \in U^* \ : \ \lim_{t\to-\infty} \phi^t(\breve{z}, \breve{E}) = (z^*, E^*), \text{ and } \phi^t(\breve{z}, \breve{E}) \in U^*, \ t \geq 0 \right\},$$

for some neighborhood U^* of (z^*, E^*).

In this respect, we are interested in integrating system (13)-(14) and simulating the stable manifold of the stationary state. Since the initial value z_0 is not available, integrating forward in time should require a shooting procedure (see [21], [22]). Anyway it is well-known that, when the computed value for z_0 is not accurate enough, then the discrete solution could exponentially diverge from the stable manifold.
As an alternative, we adopt another approach which deals with backward integration in time. Thus, time is reversed and the variables

$$\underline{E}(t) := E(-t), \quad \underline{z}(t) := z(-t),$$

are considered. The dynamics is given by

$$\dot{\underline{E}}(t) = -F(\underline{z}(t), \underline{E}(t)), \tag{20}$$
$$\dot{\underline{z}}(t) = -G(\underline{z}(t), \underline{E}(t)). \tag{21}$$

The stable manifold $\mathcal{W}^s_{loc}$, which has been already introduced, is equivalent to the unstable manifold of this reversed system. Thus, the solution $(E(t), z(t))$ of (13)-(14) on the stable manifold has a corresponding solution $\underline{E}(t), \underline{z}(t)$ for (20)-(21) on the unstable manifold, with the same trajectory in reversed direction. In this framework, the method exploits the Manifold Theorem and consists of the following steps:

- evaluate the saddle point (z^*, E^*);
- choose an initial pair $(\underline{z}_0, \underline{E}_0)$, close to (z^*, E^*) along the tangent direction

$$\underline{z}_0 = z^* + \frac{v^1_s}{v^2_s}\epsilon,$$
$$\underline{E}_0 = E^* + \epsilon,$$

  where $\epsilon \in \mathbb{R}$ is a given parameter, v^1_s and v^2_s are the entries of an eigenvector corresponding to the negative eigenvalue of the Jacobian $\mathcal{J}^*$, which generates the eigenspace $\mathcal{S}^s$ of the linearized system;
- approximate the solution of system (20)-(21) on a suitable finite time horizon $[0, \underline{t}]$ such that $\underline{E}(\underline{t}) = E_0$ and $\underline{z}(\underline{t}) = z_0$;
- reverse time again and provide

$$E(t) = \underline{E}(-t), \quad z(t) = \underline{z}(-t).$$

This approach can be considered as indirect, since it relies on the integration of the necessary optimality conditions. The code is implemented in Matlab environment. Precisely, the stationary state is evaluated by means of the `fsolve` built-in function with accuracy 10^{-8} and system (20)-(21) is solved by the standard integrator `ode45`. Moreover, we set $\epsilon = 10^{-6}$ in our simulations.

5.2. The "direct method" description

We adopt the numerical algorithm proposed in [23], where a s-stage Runge-Kutta scheme (a_{kj}, b_k, c_k) is exploited in order to describe the dynamical evolution of the variables. This numerical algorithm is able to preserve the same qualitative features of the exact solution and to provide a high order accuracy in the approximation.

The basic idea is to impose that the discrete model preserves the same equilibria of the underlying continuous-time problem. In this respect, the presence of the discount term $\mu(t) := e^{-\sigma t}$ in the objective function can represent a challenge for achieving the expected accuracy of the approximated solution; indeed, suitable approximations of the exponential function are required in order to avoid numerical instability due to possible oscillations arising in the solution itself.

The time horizon is discretized by means of two sets of temporal nodes $t_{n+1} = t_n + \Delta$, $t_{n_k} = t_n + c_k\Delta$ $(k = 1, \dots, s)$ that are obtained by time-step length Δ. As usual, we assume that the state variable $E(t)$ falls in the neighborhood of one of its stationary equilibria E^* at $t > t_N$, where N is a given index. Under this assumption, the control variable reaches the stationary value $L^*(E^*) = 1 - E^*(\overline{E} - E^*)/(\eta a)$, for $t > t_N$, arising from condition $f(L^*(E^*), E^*) = 0$. Thus, it follows that

$$\int_{t_N}^{\infty} e^{-\sigma t}\Pi(L(t), E(t))\ dt \approx \frac{e^{-\sigma t_N}}{\sigma}\Pi(L^*(E^*), E^*).$$

As a consequence, the infinite horizon objective function may be approximated by the finite horizon model

$$\max_{L} \int_0^{t_N} e^{-\sigma t}\Pi(L(t), E(t))\, dt + \frac{e^{-\sigma t_N}}{\sigma}\Pi(L^*(E^*), E^*),$$

joint with the dynamic constraint on the state variable. We introduce the set $\{L_{n_k}\}$ of nodal approximations of the control variable at each t_{n_k}; moreover, two sequences $\{\mu_n\}$ and $\{\mu_{n_k}\}$, different from zero, are defined for approximating the exponential values $\mu(t_n)$, $\mu(t_{n_k})$. Then the following discrete model is stated:

$$\max_{L_{n_k}} \Delta \sum_{n=0}^{N-1}\sum_{k=1}^{s} b_k\mu_{n_k}\,\Pi(L_{n_k}, E_{n_k}) + \frac{\mu_N}{\sigma}\,\Pi(1 - E_N(\overline{E} - E_N)/(\eta a), E_N), \tag{22}$$

subject to

$$\begin{aligned} E_{n+1} &= E_n + \Delta\sum_{k=1}^{s} b_k f(L_{n_k}, E_{n_k}), \qquad n = 0, \dots, N-1,\ E_0 = E(0), \\ E_{n_k} &= E_n + \Delta\sum_{j=1}^{s} a_{kj} f(L_{n_j}, E_{n_j}), \qquad k = 1, \dots, s, \end{aligned} \tag{23}$$

with $\{\mu_n\}$ and $\{\mu_{n_k}\}$ given by the recursive formula

$$\begin{aligned} \mu_{n+1} &= \mu_n - \sigma\Delta\sum_{k=1}^{s} b_k\mu_{n_k}, \qquad n = 0, \dots, N-1,\ \alpha_0 = 1, \\ \mu_{n_k} &= \mu_n - \sigma\Delta\sum_{j=1}^{s} \hat{a}_{kj}\mu_{n_j}, \qquad k = 1, \dots, s, \end{aligned} \tag{24}$$

where $\hat{a}_{kj} = b_j(1 - a_{jk}/b_k)$, for each j, k. It is possible to prove that approximation (24) for the exponential nodal values is chosen in order to satisfy the so-called steady-state invariance property (see [24]). More precisely, the following result holds.

Proposition 5. *Suppose $b_k \neq 0$ for each $k = 1, \ldots, s$. Under the assumption that μ_n and μ_{n_k} are nonzero values, any stationary solution of the continuous-time problem (7) is a stationary solution of the discrete-time model (22)-(23)-(24).*

Proposition 5 can be proved by exploiting the first order optimality conditions for the nonlinear programming problem (22)-(23)-(24) and analyzing the behavior of its solution at the stationary equilibrium. Here we omit the proof since it has been developed in [23], where more details can be found about the method and its features. For the sake of completeness, we would only remark that the iterative scheme (23)-(24) corresponds to the discretization of the differential system

$$\begin{aligned} \dot{E}(t) &= f(L(t), E(t)), \qquad E(0) = E_0, \\ \dot{\mu}(t) &= -\sigma\mu(t), \qquad \mu(0) = 1, \end{aligned}$$

by coupling two different Runge-Kutta solvers: the state variable $E(t)$ is discretized by the Runge-Kutta method (a_k, b_k, c_k) and the exponential approximation is obtained by another Runge-Kutta scheme $(\hat{a}_k, b_k, c_k)$, where each coefficient $\hat{a}_k$ satisfies the relationship

$$\hat{a}_{kj} = b_j(1 - a_{jk}/b_k),$$

which is known in literature as "symplecticity condition". We can also say that a so-called *symplectic partitioned Runge-Kutta scheme* (a_k, b_k, c_k)-$(\hat{a}_k, b_k, c_k)$ is adopted for the numerical approximation of variables $E(t)$ and $\mu(t)$ in the previous differential system. Some symplectic partitioned Runge-Kutta integrators have been exploited in the field of the applications to finite horizon optimal control in other papers such as [25] and [26]. Moreover, the theory about the accuracy order for any symplectic partitioned Runge-Kutta method is well-stated in literature (see, for instance, [27], [25], [28]). In this respect, for our numerical experiments, in the sequel we exploit a pair with high order accuracy given by the *classical Runge-Kutta method* $(a_k, b_k, c_k)_{k=1,\ldots,4}$ (see [29]) with tableau

0				
1/2	1/2			
1/2	0	1/2		
1	0	0	1	
	1/6	1/3	1/3	1/6

which performs an explicit and cheap approximation of the state variable $E(t)$ and is joint with its symplectic counterpart $(\hat{a}_k, b_k, c_k)_{k=1,\ldots,4}$ with tableau

0	1/6	−2/3	1/3	1/6
1/2	1/6	1/3	−1/6	1/6
1/2	1/6	1/3	1/3	0
1	1/6	1/3	1/3	1/6
	1/6	1/3	1/3	1/6

that provides an implicit discretization for the exponential function $\mu(t)$ and avoids spurious and unstable oscillations in the discrete solution, without any restriction on the choice of the time-step length Δ. The resulting numerical scheme is defined as

$$\max_{L_{n1}, L_{n2}, L_{n3}, L_{n4}} \frac{\Delta}{6} \sum_{n=0}^{N-1} \mu_{n+1} S_n + \frac{\mu_N}{\sigma} \Pi(1 - E_N(\overline{E} - E_N)/(\eta a), E_N), \tag{25}$$

subject to

$$
\begin{aligned}
&S_n = \left(1 + h + \frac{h^2}{2} + \frac{h^3}{4}\right)\Pi_1 + \left(2 + h + \frac{h^2}{2}\right)\Pi_2 + (2+h)\Pi_3 + \Pi_4,\\
&E_{n+1} = E_n + \frac{\Delta}{6}(f_1 + 2f_2 + 2f_3 + f_4), \qquad E_0 = E(0),\\
&E_{n1} = E_n, \quad E_{n2} = E_n + \frac{\Delta}{2}f_1, \quad E_{n3} = E_n + \frac{\Delta}{2}f_2, \quad E_{n4} = E_n + \Delta f_3,\\
&\mu_{n+1} = \mu_n \left(1 + h + \frac{h^2}{2} + \frac{h^3}{6} + \frac{h^4}{24}\right)^{-1}, \qquad \mu_0 = 1,
\end{aligned}
$$

where $h = \sigma\Delta$, $\Pi_i = \Pi(L_{ni}, E_{ni})$, $f_i = f(L_{ni}, E_{ni})$ for $i = 1, \ldots, 4$. This method is featured by fourth order accuracy in the approximation and it preserves the steady-state invariance, since it is possible to verify that the assumptions in Proposition 5 are satisfied by the adopted scheme in correspondence with any value for Δ. Discrete model (25) has been implemented in Matlab environment; in particular, the optimization process has been performed by means of the Matlab `fmincon` built-in function.

6. Numerical experiments

In the following numerical tests, the parameters of interest are set as follows

$$\alpha = 0.65,\ \gamma = 0.65,\ \delta = 0.3655,\ r = 0.255,\ \sigma = 0.25.$$

The values for $\overline{E}$ (the carrying capacity of the environmental resource) and η (the pollution rate of the industrial sector) change over all the cases we consider in the sequel. Figures 4 show the stable manifolds of the equilibrium points, which are obtained setting $\eta = 0.014$ and varying the parameter $\overline{E}$. Saddle points and repellors are denoted by squares and dots, respectively.

Notice that, when the value of $\overline{E}$ is sufficiently high (see, for instance, Figure 4(a)), then there exists a unique stationary state $E^* = \overline{E}$, $L^* = 1$. In correspondence with this point, the stock of the natural resource is equal to its carrying capacity $\overline{E}$ (i.e. to the maximum sustainable level) and the representative L-agent allocates all her time endowment (assumed to be equal to 1) in the production of the resource-dependent sector; as a consequence, according to (5), the external investment K_I is equal to 0. In the same Figure 4(a), we consider the dynamics that moves along the transition path which approaches the point $E^* = \overline{E}$, $L^* = 1$ from the left. In this respect, when the stock E of the natural resource is sufficiently low in a suitable neighbourhood of the origin, then the labor employed in the local sector is equal to 1 and, therefore, $K_I = 0$. The consequence is an increase in E (the local sector has no impact on E). When E moves on the left and reaches a sufficiently high value, then L decreases (that corresponds to increasing K_I); after that, L definitively increases. It is worthwhile noting that $L = 1$ holds in two different cases: either when E is low enough and near to 0 or when E is sufficiently high in a neighbourhood of $\overline{E}$. In the first case, $L = 1$ is chosen to avoid the complete depletion of the environmental resource (even though the productivity of L in the local sector is low, since E low); in the second case, $L = 1$ is chosen because the productivity in the resource-dependent sector is high with respect to the wage rate in the industrial sector. The scenario described in Figure 4(a) represents the context where the economy is endowed with a relatively high value of $\overline{E}$; in this case, the external investment K_I may be only observed along the transition path, while the economy becomes "specialized" in the resource-dependent sector when E is near to the value $\overline{E}$. The other Figures 4(b)-4(c)-4(d) can be interpreted in a similar way. Figure 4(b) shows a bi-stable regime: both the equilibrium points C and $(\overline{E}, 1)$ can be reached and the equilibrium selection depends on the initial value $E(0) = E_0$. Under the assumption that E_0 is sufficiently high, then the economy approaches $(\overline{E}, 1)$, where external investment is ruled out; otherwise, the economy converges to C, where the local sector coexists with the industrial one. Figure 4(c) represents another possible bi-stable regime where there exit two saddle points A and C, where the two sectors coexist (in this case, the state $(\overline{E}, 1)$ is not an equilibrium point). The bi-stable regimes in Figures 4(b)-4(c) are observed for "intermediate" values of the carrying capacity $\overline{E}$. When $\overline{E}$ becomes low enough, then the case

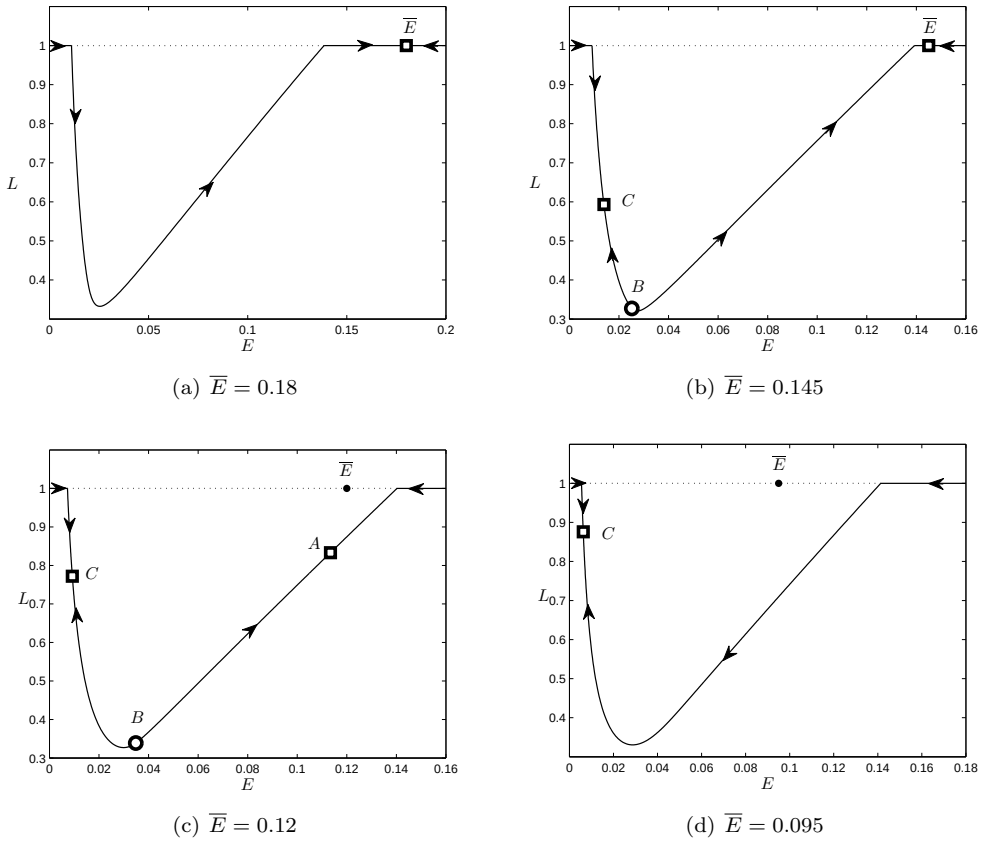

(a) $\overline{E} = 0.18$ (b) $\overline{E} = 0.145$

(c) $\overline{E} = 0.12$ (d) $\overline{E} = 0.095$

Figure 4: Stable manifolds of the saddle points, obtained varying the parameter $\overline{E}$, which measures the carrying capacity of the environmental resource.

illustrated in Figure 4(d) holds, where there exists a unique saddle point C characterized by a low value for E and a high value for L (thus, we have a low value for K_I).

In addition, the dynamics of E and K_I along the stable manifolds of the saddle points A and C, in the bi-stable regime shown in Figure 4(c), is provided in Figure 5; notice that, in the equilibrium A, the values for E and L are higher than in C, while the opposite case holds for the value of the external investment K_I (according to (5)).

Applying the "indirect method"already described in the previous Section, we also developed other numerical tests in order to evaluate the effects of an increase in the pollution rate of the industrial sector η. The simulations in Figures 6 were obtained by setting $\overline{E} = 0.095$ and varying the value of η. Notice that, if the value of η is low (Figure 6(a)), a bi-stable regime is observed; however, when the value of η becomes sufficiently high (Figure 6(c)), then we observe a dynamic regime where the point $(\overline{E}, 1)$ is the unique existing stationary state and the economy tends to specialize in the resource-dependent sector.

The remaining figures show the results obtained applying the "direct method". We set $\overline{E} = 0.12$ and $\eta = 0.014$; under this choice, the phase portrait is that given in Figure 4(c). Figures 7-10 represent the time evolution of the state and control variables in correspondence with the initial conditions $E(0) = 0.004$, $E(0) = 0.025$, $E(0) = 0.07$ and $E(0) = 0.15$, respectively. All the results have been obtained by employing the same time-step length $\Delta = 0.5$; in order to have an even representation, the figures show the dynamics of control and state variables with the same number of nodes. The time evolution paths starting from $E(0) = 0.004$ and $E(0) = 0.025$ approach the equilibrium C (see Figures 7-8), while the ones starting from $E(0) = 0.07$ and $E(0) = 0.15$ converge to the equilibrium A (see Figures 9-10). It is worth to note that the time evolution of the state variable E is always monotonic (see also Figures 4 and 6). It implies that the evolution of E cannot be represented by a *U-shaped* path along which the value for E is firstly decreasing and then

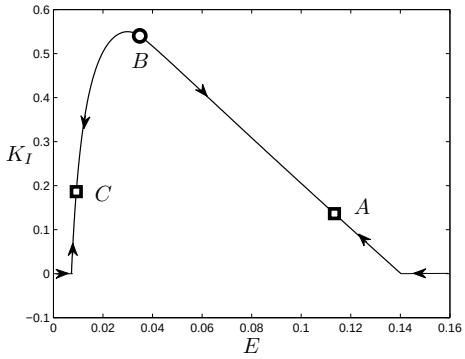

Figure 5: The evolution of E and K_I along the stable manifolds of the saddle points A and C, in the bi-stable regime shown in Figure 4(c).

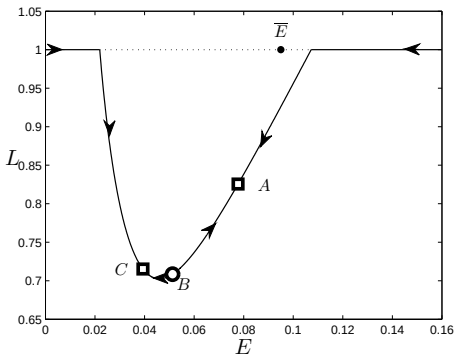

(a) $\eta = 0.024$

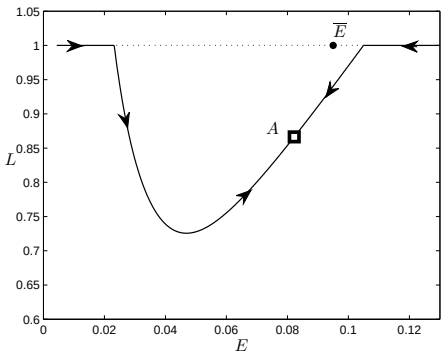

(b) $\eta = 0.025$

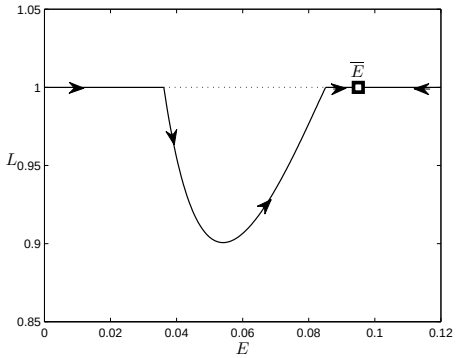

(c) $\eta = 0.028$

Figure 6: Stable manifolds of the saddle points, obtained varying the parameter η, which measures the pollution rate of the industrial sector.

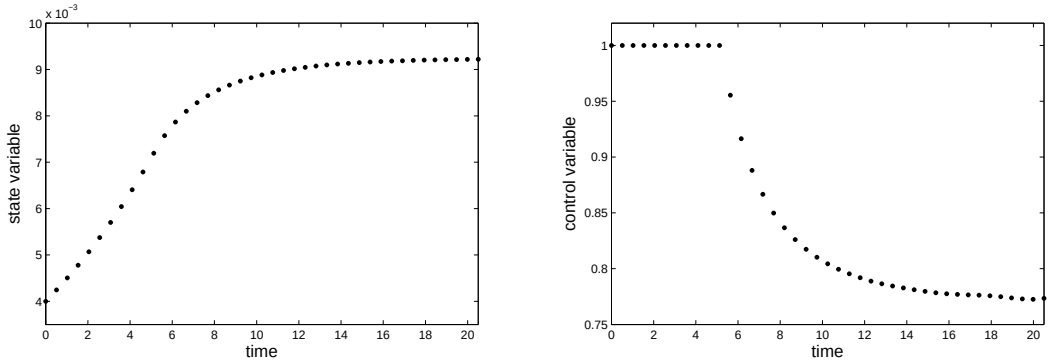

Figure 7: Evolution dynamics for the state variable (left) and the control (right) in correspondence with $E(0) = 0.004$.

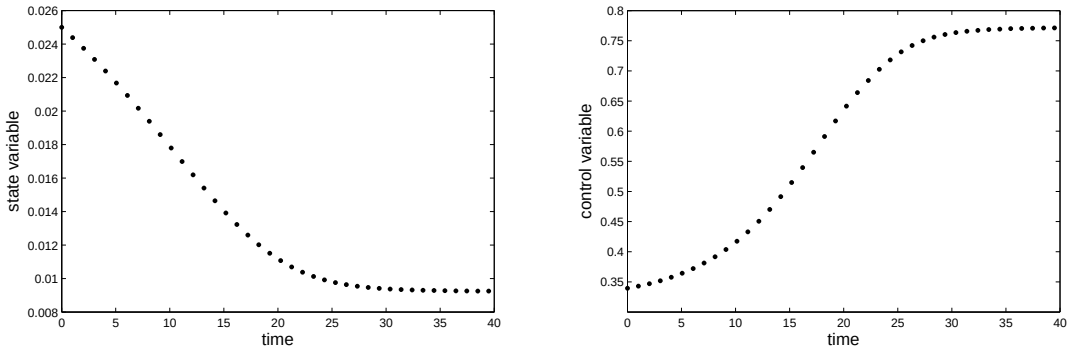

Figure 8: Evolution dynamics for the state variable (left) and the control (right) in correspondence with $E(0) = 0.025$.

definitively increasing. This means that our model does not generate an *environmental Kuznets curve* (see, among the others, [30], [31], [32], [33]). The *U-shaped* path is usually observed in models where the accumulation process of the industrial capital depends on the consumption/investment decisions of economic agents rather than on external capital inflows, as it happens in our model.

We would remark that the other cases in Figures 4(a)-4(b)-4(d) have been also reproduced by exploiting the direct method. All the solutions provided by the direct approach and the indirect one are in perfect agreement. For that reason and for the sake of brevity, we do not show all the time evolution dynamics and prefer to provide the stable manifolds in the space (E, L) in Figures 4. In addition, we remark again that the use of the two different procedures which provide the same discrete approximations validates the results we show so far.

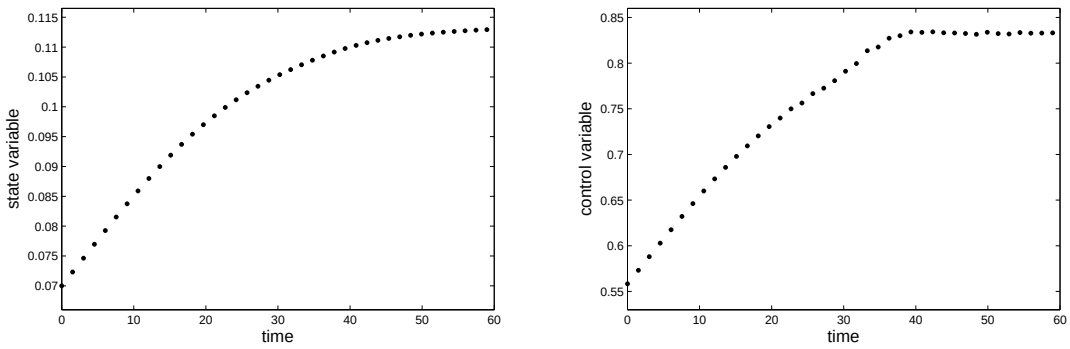

Figure 9: Evolution dynamics for the state variable (left) and the control (right) in correspondence with $E(0) = 0.07$.

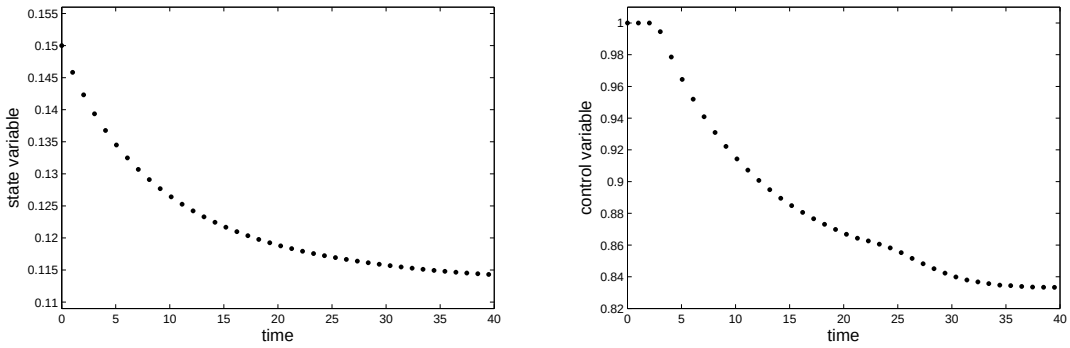

Figure 10: Evolution dynamics for the state variable (left) and the control (right) in correspondence with $E(0) = 0.15$.

7. Conclusions

We have analyzed an economic growth model with three factors of production -labor, a renewable natural resource and physical capital- and two sectors -the "industrial sector" and the "local sector". Physical capital is specific to the industrial sector whereas the natural resource is specific to the local sector. External investors invest in the industrial sector as long as the return on capital which is invested is higher than in the other economies. The activity of the industrial sector causes a negative impact on the environmental resource. In this framework, we have analyzed the economic dynamics under the assumption that the labour allocation between the two sectors of the economy is optimal, that is, it maximizes the discounted flow of the local population revenues.

Our findings show that, in this kind of economy, the external investments may give rise to path-dependent dynamics. More specifically, three stationary states A, B and C may exist; A and C are saddle points while B is a repellor (see Figure 4(c)); In A and C the two sectors of the economy coexist and the equilibrium selection depends on the initial condition for the stock of the environmental resource $E(0)$. Another bi-stable regime that may be observed is the one shown in Figure 4(b), with the repellor B separating the stable manifold of C from the stable manifold of a stationary state $(E, L) = (\overline{E}, 1)$ where the investment in physical capital is $K_I = 0$; therefore, the economy is specialized in the resource-dependent sector. These two cases of path-dependence emerge only for intermediate values of the carrying capacity $\overline{E}$ of the environmental resource and for sufficiently low values of the rate η of the environmental impact by the incoming activities. When these conditions are not satisfied, then a unique stationary state exists. For instance, in Figure 4(a) we show a case when the carrying capacity $\overline{E}$ is sufficiently high and the unique existing stationary state is $(E^*, L^*) = (\overline{E}, 1)$, therefore the economy is specialized in the resource-dependent sector. On the other hand, Figure 4(d) corresponds to a low value for the carrying capacity $\overline{E}$, then there exists a unique stationary state where the two sectors coexist.

The numerical analysis of the model has pointed out two further features of the dynamics: 1) The control variable L, which measures the optimal labor input in the resource-dependent sector, assumes the value 1 (i.e. the economy specializes in the resource dependent sector) either if the stock E is low enough or if it is sufficiently high; however, in the first case, the same choice $L = 1$ avoids the complete depletion of the environmental resource (the resource-dependent sector has no impact on E), while in the second case, the choice $L = 1$ is motivated by the high productivity of labor in the resource-dependent sector. 2) The state variable E, which measures the stock of the environmental resource, has monotonic time evolution paths (see Figures 7-10). This implies that the stock E cannot follow *U-shaped* paths along which E is initially decreasing and then definitively decreasing. This result suggests that if the capital accumulation process is driven by external investments only, then the so called Environmental Kuznets Curve cannot be observed (in a context in which labor allocation is optimal).

We sum up that our results show how the openness to external investments does not exclude both environmental sustainability and an improvement in the welfare of local population even when the incoming capitals are invested in polluting activities and they flow towards economies that are highly dependent on natural capital. The carrying capacity $\overline{E}$, the initial stock of natural capital

$E(0)$ and the rate of environmental impact of the external sector η play a key role in determining the transition towards a diversified economic structure. The analyzed model can be generalized by assuming that also local economic agents can accumulate physical capital; we leave this extension of our model to future research.

Acknowledgement

The authors would like to thank the anonymous referees for their comments, that have been useful in order to improve the paper.

[1] Y.F. Lee, A.Y. So, The role of the sectoral composition of foreign direct investment on growth. In Lee, Y.F., So, A.Y., editors, Asia's environmental movements: comparative perspectives. M. E. Sharpe, Armonk & New York, 1999.
[2] J. Martines-Alier, The environmentalism of the poor: a study of ecological conicts and valuation, Edward Elgar Pub., Cheltenham, UK, 2002.
[3] A. De Janvry, R. Garcia, Rural poverty and environmental degradation in latin america: causes, effects and alternative solutions. S88/L.3/Rev.2,Rome: IFAD. 1988
[4] J. Heath, H. Binswanger, Natural resource degradation effects on poverty and population growth are largely policy-induced: the case of Colombia, Environment and Development Economics 1(1) (1996) 65–86.
[5] K. M. Chomitz, At loggerheads? Agricultural expansion, poverty reduction, and environment in tropical forests. World Bank Policy Research Report,Washington D.C. 2008.
[6] E. C. Economy, The river runs black: the environmental challenge to China's future. Cornell University Press, Ithaca &London, 2004.
[7] World Bank, Cost of pollution in China, economic estimates of physical damages. The World Bank, Washington, 2007.
[8] N. Chang, The empirical relationship between openness and environmental pollution in china, Journal of Environmental Planning and Management 55(6) (2012) 783-796.
[9] S. Boopathi, M. Rameshkumar, Economic and environmental consequences of the impact of industrial pollution: A case experience of domestic rural water supply, International Journal of Ecological Economics & Statistics 20 (2011) 75-94.
[10] S. Bartolini, L. Bonatti, Environmental and social degradation as the engine of economic growth, Ecological Economics 43(1) (2002)1-16.
[11] A. Antoci, S. Bartolini, Negative externalities, defensive expenditures and labour supply in an evolutionary context, Environment and Development Economics 9(5) (2004) 591-612.
[12] A. Antoci, P. Russu, E. Ticci, Environmental externalities and immiserizing structural changes in an economy with heterogeneous agents, Ecological Economics 81(C) (2012) 80-91.
[13] A. Antoci, P. Russu, E. Ticci, Rural poor economies in front of foreign investors: an opportunity or a risk? PLOSE ONE (2014). DOI 10.1371/journal.pone.0114703.
[14] E. B. Barbier, Poverty, development, and environment, Environment and Development Economics 15(6) (2010) 635-660.
[15] R. E. Lopez, Sustainable economic development: on the coexistence of resourcedependent and resource-impacting industries, Environment and Development Economics 15 (2010) 687–705.
[16] S. M. Aseev, Infinite-horizon optimal control with applications in growth theory, Steklov Mathematical Institute, Moskow Russia (2009) 1-148.
[17] M. Brunner, H. Strulik, Solution of perfect foresight saddlepoint problems: a simple method and application, Journal of Economic Dynamcs & Control 26 (2006) 737-753.
[18] J. Carr, Applications of center manifold theory. New York: Springer, 1981.
[19] J. Marsden, M. McCracken, Hopf bifurcation and its applications, New York: Springer, 1976 .
[20] A. Kelley, The stable, center-stable, center, center-unstable, unstable manifolds, Journal of Differential Equations 3(4) (1967) 546-570.
[21] D. Lipton, J. M. Poterba, J. D. Sachs, L. H. Summers, Multiple shooting in rational expectation models, Econometrica, 50 (1982) 1329-1333.
[22] U. M. Ascher, L. R. Petzold, Computer Methods for Ordinary Differential Equations and Differential-Algebraic Equations. Philadelphia: Society for Industrial and Applied Mathematics, 1998.
[23] S. Ragni, F. Diele, C. Marangi, Steady-state invariance in high-order Runge-Kutta discretization of optimal growth models. Journal of Economic Dynamics and Control 34 (2010) 1248-1259.
[24] J. Mercenier, P. Michel, Discrete-time finite horizon approximation of infinite horizon optimization problems with steady-state invariance. Econometrica 62(3) (1994) 635-656.
[25] J. F. Bonnans, J. L. Varin, Computation of order conditions for symplectic partitioned Runge-Kutta schemes with application to optimal control, Numerische Mathematik 103(1) (2006) 1-10.
[26] F. Diele, C. Marangi, S.Ragni, Exponential Lawson integration for nearly Hamiltonian systems arising in optimal control, Mathematics and Computers in Simulations 81 (2011) 1057-1067.
[27] W. W. Hager, Runge-Kutta methods in optimal control and the transformed adjoint system, Numerische Mathematik 87 (2) (2000) 247-282.
[28] E. Hairer, C. Lubich, G. Wanner, Geometric Numerical Integration. Springer-Verlag, Berlin, 2002.
[29] J. D. Lambert, Numerical Methods for Ordinary Differential Systems. John Wiley & Sons, Chichester, 1991.
[30] S. Borghesi, The environmental Kuznets curve: a survey of the literature, Fondazione ENI Enrico Mattei, Nota di lavoro 85.99, Milan, Italy, 1999.

[31] J. Choumert, P. C. Motel, H.K. Dakpo, Is the environmental Kuznets curve for deforestation a threatened theory? A meta-analysis of the linerature, Ecological Economics 90 (2013) 19-28.
[32] R. Duarte, V. Pinilla, A. Serrano, Is there an environmental Kuznets curve for water use? A panel smooth transition regression approach, Economic Modelling 31 (2013) 518-527.
[33] S. Farhani, S. Mrizak, A. Chaibi, C. Rault, The environmental Kuznets curve and sustainability:a panel data analysis, Energy Policy 71 (2014) 189-198.

Appendix A. Proofs

Appendix A.1. Proof of properties (P1)-(P6)

Condition (P1) is easily obtained from relationship (8). Furthermore, for each $L \in U$ we have $\eta a(1-L) \geq 0$, thus

$$f(L,E) \leq E(\overline{E}-E) \leq E\,\overline{E}.$$

It follows that

$$E \cdot f(L,E) \leq E^2\,\overline{E} \leq \overline{E}(1+E^2),$$

thus property (P2) is proved. Condition (P3) holds by setting

$$f_0(E) := E(\overline{E}-E) - \eta a, \qquad f_1(E) := \eta a.$$

Moreover, property (P4) is trivial and (P5) easily follows from relationship

$$\frac{\partial^2 \Pi}{\partial L^2}(L,E) = \alpha(\alpha-1)E^{\alpha}L^{-\alpha} \leq 0,$$

for each $0 < L \leq 1$, under the assumption that $E \in X$.

Moreover, in order to prove (P6), we fix $t > 0$ and consider $|\Pi(L,E(t))| = \Pi(L,E(t))$ for $L \in U$. Due to relationship (8) and condition $0 \leq L \leq 1$, we have

$$|\Pi(L,E(t))| \leq C_0^{\alpha}L^{1-\alpha} + a(1-\gamma)(1-L) \leq C_0^{\alpha} + a(1-\gamma),$$

and

$$\max_L |\Pi(L,E(t))| \leq C_0^{\alpha} + a(1-\gamma).$$

Thus, we set

$$\nu(t) = e^{-\sigma t}(C_0^{\alpha} + a(1-\gamma)).$$

It is evident that $\nu(t) \to 0$ as $t \to +\infty$ and

$$e^{-\sigma t}\max_{L\in U} |\Pi(L,E(t))| \leq \nu(t).$$

Moreover, for any $T > 0$ we define

$$\omega(T) = \int_T^{+\infty} \nu(s)\,ds = \frac{e^{-\sigma T}}{\sigma}(C_0^{\alpha} + a(1-\gamma)).$$

We have $\omega(T) \to 0$ as $T \to +\infty$ and

$$\int_T^{+\infty} e^{-\sigma t}|\Pi(L(t),E(t))|\,dt \leq \omega(T).$$

Under this argument, property (P6) is completely proved.

Appendix A.2. Proof of Proposition 3

In order to assure the existence of three inner stationary states, we require that the curve $\mathcal{C}_F$ crosses the line $z = \overline{z}$ in Ω and the minimum point for $\mathcal{C}_G$ is located on $(z = 1/\overline{E}, E = 0)$. Those requirements are equivalent to have:

- $\widetilde{z} < \overline{z}$, and $\sqrt{a\eta} < \overline{E}$,

- $\widetilde{z}\overline{E} = 1$, and $\varphi(\widetilde{z}) = 0$.

In this way, condition (16) is obtained in a direct way. In addition, by exploiting assumption $\varphi(\widetilde{z}) = 0$, we have (17). Moreover, $\sqrt{a\eta} < \overline{E}$ yields

$$\eta < \frac{1}{a\overline{z}^2}, \tag{A.1}$$

which has to be coupled with the following condition

$$\eta - \frac{2}{\sqrt{a}\,\overline{z}(1-\alpha)^{\frac{1}{\alpha}}}\sqrt{\eta} + \frac{1}{a\,\overline{z}^2(1-\alpha)^{\frac{1}{\alpha}}} > 0, \tag{A.2}$$

that arises from $\widetilde{z} < \overline{z}$. It is not so difficult to verify that the solution to system (A.1)-(A.2) with respect to η consists of the positive values which satisfy condition (18). In this way, the result is completely proved.

Appendix A.3. Proof of Proposition 4

Assume the existence of three stationary points $A(z_A^*, E_A^*)$, $B(z_B^*, E_B^*)$ and $C(z_C^*, E_C^*)$, with $z_A^* < z_B^* < z_C^*$. In the proof of Proposition 2 we have already noticed that the point C is on the lower branch of the curve $\mathcal{C}_F$, on the strip defined by the interval $[\widetilde{z}, +\infty[$. On the other hand, A and B lie on the strip defined by the interval $[\widehat{z}, \widetilde{z}]$. The point B is again on the lower branch of $\mathcal{C}_F$, while A may be located either on the upper branch or on the lower one (see Figure 3).

As a first step, we assume that the state A is on the upper branch, as it is shown in Figure 3(a), since the case described in Figure 3(b) can be analyzed in a similar way and the same result can be obtained. The basic idea in this argument exploits the slopes of the curves $\mathcal{C}_F$ and $\mathcal{C}_G$ at their crossing points A, B and C. Those slopes provide insights about the sign of the derivatives of functions $F(z, E)$ and $G(z, E)$ which are needed to evaluate the sign of $\mathcal{T}$ and $\mathcal{D}$ in $\mathcal{P}(\lambda)$; in this way, the sign of the Jacobian matrix eigenvalues is known and a stability analysis can be carried out for the states A, B and C.
In this respect, we notice that the slope of the curve $\mathcal{C}_F$ is given by

$$m_F(z, E) = -\frac{F_z(z, E)}{F_E(z, E)},$$

at any given point $(z, E) \in \mathcal{C}_F$. It is obtained by applying the implicit function theorem in order to solve equation $F(z, E) = 0$. Indeed, since F is a continuously differentiable function, then it is possible to consider a function $\psi(z)$ whose graph $(z, \psi(z))$ is the set of all the points (z, E) such that $F(z, E) = 0$; in addition, $\psi(z)$ is smooth and $\psi'(z) = -F_z(z, \psi(z))/F_E(z, \psi(z))$.
In the same way, it is possible to prove that the slope of the curve $\mathcal{C}_G$ is given by

$$m_G(z, E) = -\frac{G_z(z, E)}{G_E(z, E)},$$

at any given point $(z, E) \in \mathcal{C}_G$. The stability analysis can be developed as in the following items:

- At the stationary state C the curve $\mathcal{C}_F$ is decreasing with respect to z and $\mathcal{C}_G$ is increasing; therefore, we have

  $$m_F(z_C^*, E_C^*) < 0, \qquad m_G(z_C^*, E_C^*) > 0.$$

  Since $F_z(z, E) = \eta a\overline{E} > 0$ and $G_E(z, E) = 2az(1-\gamma)(z^\alpha - \overline{z}^\alpha)/(\alpha(1-\alpha)) > 0$ at any point, then it follows that

  $$F_E(z_C^*, E_C^*) > 0, \qquad \text{and} \qquad G_z(z_C^*, E_C^*) < 0;$$

  thus $\mathcal{D} < 0$ in $\mathcal{P}(\lambda)$. The eigenvalues related to C change their sign; therefore, this stationary state represents a saddle point.

- At the stationary state B the curves $\mathcal{C}_F$ and $\mathcal{C}_G$ are both decreasing and the slope for $\mathcal{C}_G$ is greater than the other one, according to their absolute value:

$$m_F(z_B^*, E_B^*) < 0, \qquad m_G(z_B^*, E_B^*) < 0, \qquad |m_F(z_B^*, E_B^*)| < |m_G(z_B^*, E_B^*)|.$$

  Then, we have

$$F_E(z_B^*, E_B^*) > 0, \qquad G_z(z_B^*, E_B^*) < 0, \qquad \text{and} \qquad \frac{F_z(z_B^*, E_B^*)}{F_E(z_B^*, E_B^*)} < \frac{G_z(z_B^*, E_B^*)}{G_E(z_B^*, E_B^*)};$$

  thus $\mathcal{D} > 0$ and $\mathcal{T} > 0$ in $\mathcal{P}(\lambda)$. The eigenvalues related to B preserve their sign; therefore, this equilibrium represents a repellor.

- At the stationary state A the curve $\mathcal{C}_F$ increases and $\mathcal{C}_G$ decreases; therefore, we have

$$m_F(z_A^*, E_A^*) > 0, \qquad m_G(z_A^*, E_A^*) < 0.$$

  It follows that

$$F_E(z_A^*, E_A^*) < 0, \qquad \text{and} \qquad G_z(z_A^*, E_A^*) > 0;$$

  thus $\mathcal{D} < 0$ in $\mathcal{P}(\lambda)$. The eigenvalues related to A change their sign; therefore, this stationary state represents a saddle point.

As we already pointed out, similar arguments can be developed when the point A lies on the lower branch of $\mathcal{C}_F$ (see Figures 3(b) and 3(c)): the same results are obtained as in the previous discussed case, where A was on the upper branch.